Experimental Study on Characteristics of Two-Phase Flow through a Bypass Orifice Expansion Device

Jong-Min Choi* and Yong-Chan Kim**

Key words : Bypass orifice, Straight orifice, Inverter-driven heat pump

Abastract

To establish optimum cycle of the inverter-driven heat pump with a variation of frequency, the bypass orifice, which was a short tube having a bypass hole in the middle, was designed and tested. Flow characteristics of the bypass orifice were measured as a function of orifice geometry and operating conditions. Flow trends with respect to frequency were compared with those of short tube orifices and capillary tubes. Generally, the bypass orifice showed the best flow trends among them, and it would enhance the seasonal energy efficiency ratio of an inverter heat pump system. Based on experimental data, a semi-empirical flow model was developed to predict mass flow rate through bypass orifices. The maximum difference between measured data and model's prediction was within ±5%.

Nomenclature

A : Orifice cross-sectional area (㎡)
C : Discharge coefficient for orifice equation
DB : Bypass hole diameter (mm)
Din : Inlet diameter of the bypass orifice (mm)
Dout : Outlet diameter of the bypass orifice (mm)
DR : Normalized diameter
EVAP: Normalized downstream pressure
L : Orifice length (mm)
LB : Position of bypass hole from entrance of bypass orifice (mm)
$\dot{m}_s$: Mass flow rate (kg/h)
P : Pressure (kPa)

Greek Symbols

ρ : Density (kg/㎥)

Subscripts

c : Critical state

* Graduate School, Korea Univ. Seoul, Korea
** Department of Mechanical Engineering, Korea Univ. Seoul, Korea

down : Downstream
up : Upstream
sat : Saturation

1. Introduction

An inverter heat pump makes the continuous operation of a compressor possible through capacity modulation of the system utilizing frequency control. It also provides several advantages in energy conservation, capacity control and comfort of the indoor environment over a constant speed heat pump[1,2].

The capillary tube, which is suitable for systems of small capacities and advantageous in cost and reliability, is being widely used as an expansion device in the inverter heat pump. However, when applying the capillary tube to the inverter heat pump system, it is difficult to establish an optimum cycle at all frequencies. Performance degradation of the inverter heat pump system with the capillary tube was obviously observed at low frequencies[3].

An orifice(short tube orifice) are often applied to heat pump and residential air conditioner. Usage of the orifice has been increased, because of its low cost, high reliability, ease of installation and inspection, and elimination of additional check valves used for flow direction change in heat pump applications.

Aaron and Domanski[4] developed a semi-empirical flow model which could predict the mass flow rate in a short tube orifice, with subcooled conditions at the inlet of the short tube orifice. Using HFC refrigerants, Kim and O'Neal[5] made an empirical flow model to predict the performance of the short tube orifice for subcooled and two-phase conditions at the inlet of the short tube orifice.

Recently, the orifice expansion device has been widely applied to heat pump systems. Most of the previous research associated with the orifice were focused on the rigid orifice suitable for a constant speed heat pump.

In the present study, a bypass orifice expansion device simple in structure was designed by modifying the orifice (called the straight orifice). The basic characteristics of the bypass orifice were measured as a function of operating conditions and orifice geometry. Test results were compared with those for the capillary tube and the straight orifice. The flow model for bypass orifices was developed from the results of characterization tests.

2. Experimental setup and test procedure

As shown in Fig. 1, the experimental apparatus for the measurement of basic characteristics of bypass orifices was designed to allow for easy control of each operating parameters such as entrance subcooling, condensing and evaporating pressure. The mass flow rate of the refrigerant entering the test section was controlled by varying the rotational speed of the liquid pump. The degree of subcooling of the refrigerant entering the test section was regulated by controlling the temperature and the mass flow rate passing through the water heated evaporation heat exchanger. The exit pressure of the test section was set by both the temperature and the mass flow rate of the water/glycol solution in the condensation heat exchanger. After finishing series of tests for the bypass orifice, the test section was replaced with a new test section. The replacement of the test section was conducted by closing the ball valves before and after the test section to shut off the re-

frigerant flow. After changing the test section, the space between the ball valves was evacuated and new series of the tests were performed.

Figure 2 shows the test section of the bypass orifice. The bypass orifice designed in the present study was tapered toward the flow direction and had two bypass holes in the middle of the orifice. All the other configurations were identical to the straight orifice (Fig. 3) that had been widely used in the air conditioning system as an expansion device. The orifices used in this investigation are listed in Table 1.

Performance tests were executed by varying the upstream pressure, downstream pressure, and inlet subcooling. Upstream pressure

Table 1 Dimensions of tested orifices.

L (mm)	D_{in} (mm)	D_{out} (mm)	DB (mm)	LB (mm)
15	1.26	1.26	Straight Orifice	
15	1.26	1.26	0.79	7.91
15	0.99	1.37	0.73	7.87
15	1.33	0.80	0.53	7.87
15	1.36	0.91	0.52	7.85
15	1.38	0.92	0.73	7.94
15	1.39	0.94	0.56	7.86
15	1.40	0.86	0.53	7.88
15	1.43	0.91	0.50	7.87
15	1.39	0.98	0.57	5.92
15	1.37	0.92	0.56	10.36
15	1.36	0.89	0.66	7.88
15	1.38	0.92	0.56	7.92

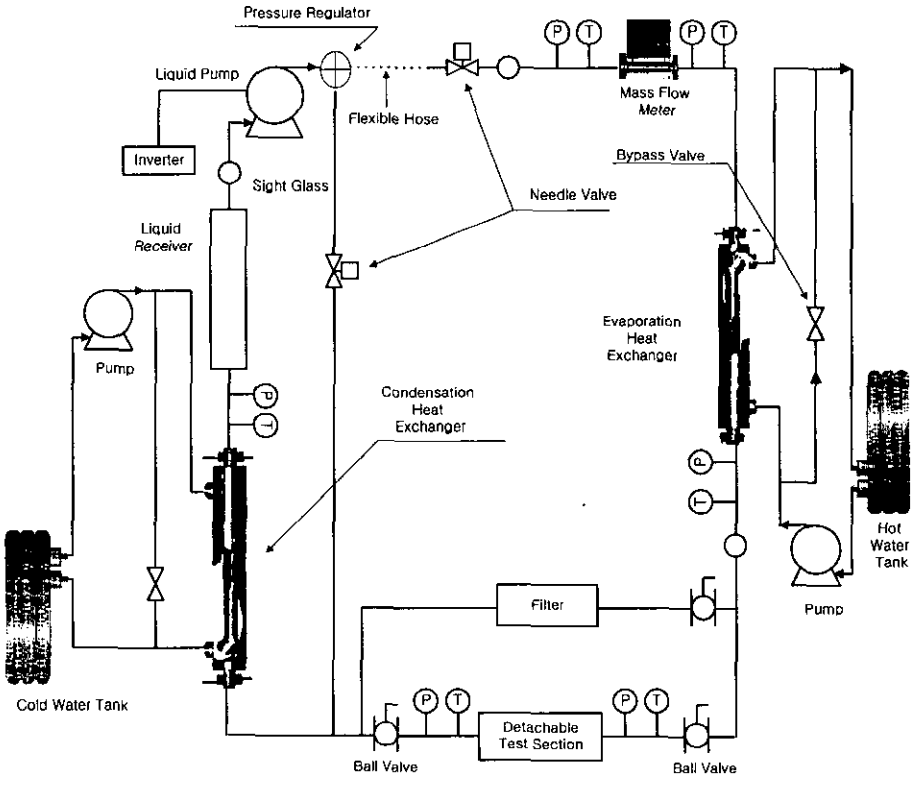

Fig. 1 Schematic of the orifice test setup.

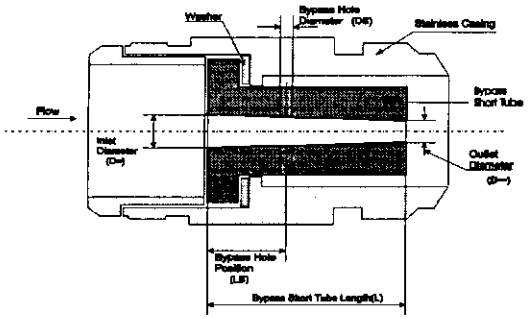

Fig. 2 Test section of the bypass orifice.

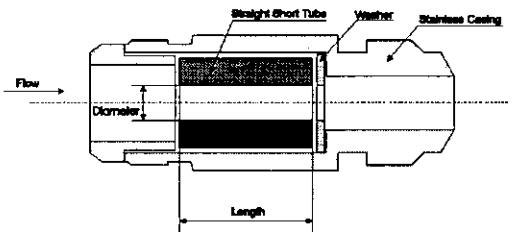

Fig. 3 Test section of the straight orifice.

was ranged from 1645 kPa to 1963 kPa, and the downstream pressure was varied below saturation pressure according to the inlet temperature. The subcooling at the entrance of the test section was varied from 1℃ to 13.9℃. Table 2 shows the test matrix for the experiment. R-22 was used as a working fluid in this study.

Temperatures, pressures, and flow rate were monitored in the test loop using a computer data acquisition system. Each sensor was calibrated to reduce experimental uncertainties and connected to the data logger. All temperature measurements were made using the copper constant thermocouple with an experimental uncertainty of ±0.1℃. Pressure transducers were used in measuring the refrigerant pressures with an estimated accuracy of ±0.4 % of full scale(3447 kPa) for the high pressure transducer, and ±0.2 % of full scale(1724 kPa) for the low pressure transducer. The refrigerant flow rate was measured with a mass flow meter, and it was calibrated with water. The accuracy of the mass flow meter was ± 0.2% of reading.

Table 2 Test conditions.

Parameters	P_{up}(kPa)	P_{down}(kPa)	T_{sub}(°C)
Conditions	1645	600	13.9
	1841	700	8.7
	1963	780	5.7
		800	1
		850	
		900	

The data were taken at steady state. Before taking the data, the controlling parameters had to be within the following limits : upstream pressure, ±7 kPa; downstream pressure, ±14 kPa; and subcooling, ±0.3℃.

3. Results and Discussion

Since the inverter heat pump is capable of covering a wide range in capacity corresponding to building load throughout the year, the wide range of refrigerant flow regulation is required as a function of frequency of the compressor. Even though the capillary tube is selected to have the best performance at the rated frequency, the inverter heat pump with the capillary tube is not able to achieve optimal performance at both low and high frequencies. For the low frequency region, the inverter heat pump showed the maximum performance when the mass flow rate was adequately decreased by increasing the capillary tube length as compared with the base capillary tube. Whereas for the high frequency region, it represented the maximum performance when the mass flow rate was increased by

decreasing the capillary tube length as compared with that of the base capillary tube[5]. Therefore, an economical expansion device which allows a large variation in mass flow rate with a change of frequency compared to the capillary tube is in demand.

In this study, the bypass orifice expansion device was designed by modifying the orifice. The basic characteristics of the bypass orifice were measured and analyzed as a function of operating conditions and geometries.

3.1 Effects of operating conditions

Figure 4 shows the effects of the downstream (evaporating) pressure on mass flow rate for three different upstream pressures. For the downstream pressure below the liquid saturation pressure corresponding to the upstream temperature, mass flow rate became relatively independent of the downstream pressure. Choked flow was observed in the bypass orifice and these trends were identical to that of capillary tubes and straight orifices[4-6]. Therefore, the system can obtain operational reliability with an application of bypass orifices.

Figure 5 represents the effects of the upstream pressure on mass flow rate. As the upstream pressure increased with a constant upstream subcooling, the mass flow rate linearly increased. As the upstream subcooling decreased, the slope of each line decreased. As the upstream pressure increases for a constant upstream subcooling, the upstream liquid density decreases due to an increase of fluid temperature, but the allowable subcooled pressure drop increased. The former tends to decrease mass flow rate, but the latter increases mass flow rate. For high subcooling, the effects of the latter were larger than those of the former. As the upstream subcooling decreased, the allowable subcooled pressure drop reduced, while the decrease of the upstream liquid density was very small.

As the upstream pressure increased from 1645 kPa to 1963 kPa, the increase of mass flow rate was 4.7 kg/h with a subcooling of 1℃. However, the increase of mass flow rate was 10.3 kg/h for subcooling of 13.9℃. The effects of the upstream pressure for the bypass orifice were consistent with those for the straight orifice[5]. However, the variation of the mass flow rate according to the upstream pressure for the bypass orifice was larger than that of the straight orifice. For the straight orifice, the sharp pressure drop occurred at

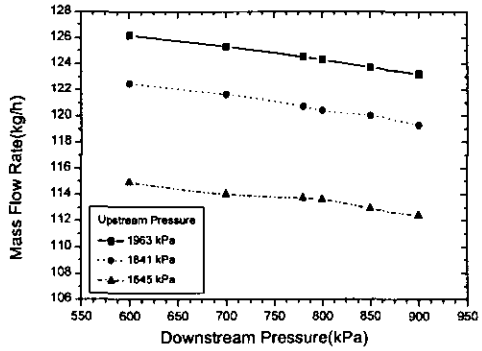

Fig. 4 Flow dependency on downstream pressure.

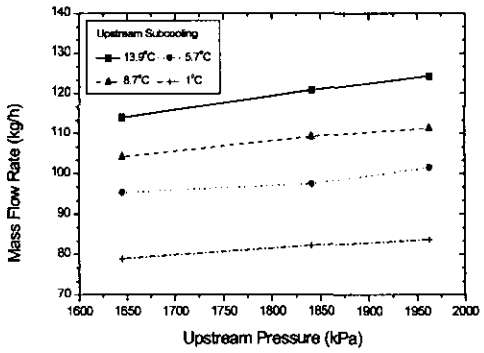

Fig. 5 Flow dependency on upstream pressure.

the entrance, and it determined mass flow rate. The bypass orifice also showed the large pressure drop at the entrance due to sharp edged contraction. However, the mass flow rate was adjusted by the interior pressure and flashing point, due to bypass holes inside the bypass orifice.

Figure 6 shows the effects of the upstream subcooling on mass flow rate. As the subcooling increases, the density and entrance pressure drop increase, while the internal pressure of the orifice decreases. The former tends to increase the mass flow rate through the main orifice, while the latter decreases the mass flow rate through the bypass hole. The increase of the major mass flow rate was larger than the decrease of the bypass mass flow rate as the upstream subcooling increased. Therefore, the total flow rate increased with an increase of the upstream subcooling.

3.2 Effects of bypass orifice geometry

Figure 7 shows the effects of upstream subcooling on mass flow rate as a function of L/D_{in}. As the L/D_{in} increased, the mass flow rate decreased at all subcooling levels. This trends were consistent with the results of Aaron and Domanski[4], and Kim[5] for the straight orifice.

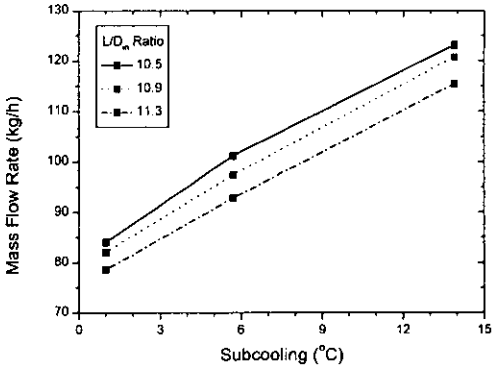

Fig. 7 Flow dependency on upstream subcooling as a function of the L/D_{in}.

As the L/D_{in} increased, flow restriction through the orifice increased, and the flashing point moved toward the inlet of the bypass orifice. Therefore, the mass flow rate decreased with an increase of L/D_{in}.

Figure 8 shows the effects of bypass hole position on mass flow rate for three different upstream pressures. As the position of the bypass hole moves toward the exit of the bypass orifice, the internal pressure of the bypass orifice decreases, and the pressure at the inlet of the bypass hole decreases. As a result, the mass flow rate through the bypass hole decreases with a movement of the by-

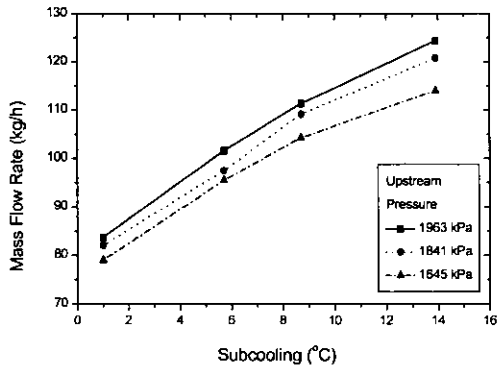

Fig. 6 Flow dependency on upstream subcooling.

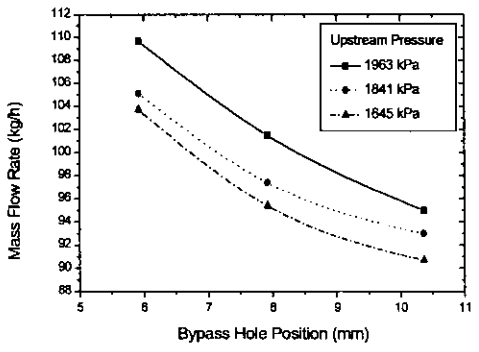

Fig. 8 Flow dependency on bypass hole position.

pass hole toward the exit. The slope of the mass flow rate of the bypass orifice with a variation of frequency can be altered by changing the location of the bypass hole.

3.3 Performance comparison of capillary tube, straight orifice, and bypass orifice.

Figure 9 shows the effects of frequency on mass flow rate for the capillary tube, the straight orifice, and the bypass orifice. The data for the capillary tube was obtained by utilizing the flow model in the literature[6]. The others were the measured data from the present experiment. The operating conditions for each frequency were selected based on the test results of the inverter heat pump with the capillary tube[3].

When the mass flow rate at the rated frequency was identically set for all of the expansion devices to provide the reference point, the slope of mass flow rate for the bypass orifice as a function of frequency was greater than that of the straight orifice or the capillary tube. The mass flow rate of the capillary tube linearly increases[7-9] corresponding to the inlet pressure and subcooling, but increases nonlinearly with respect to subcooling in the straight orifice[5]. Therefore, the slope of the mass flow rate of the straight orifice as to frequency was greater than that of the capillary tube.

The mass flow rate of the bypass orifice as a function of the inlet pressure and subcooling was similar to that of the straight orifice. However, the bypass orifice had a bypass hole, and the main hole was tapered toward flow direction. When the entrance pressure of the bypass orifice increased, the flow rate through bypass hole increased due to the followings: (1) the pressure at the inlet of the bypass hole was raised because the internal pressure of the bypass orifice increased, and (2) the subcooling at the inlet of the bypass hole increased because the flashing point moved to the exit of the bypass orifice. Therefore, the mass flow rate of the bypass orifice was also affected by the location of flashing point and internal pressure.

3.4 Effects of tapering angle

Figure 10 shows the mass flow rate as a function of tapering angle. When D_{in} is larger than D_{out}, the slope of mass flow rate vs. fre-

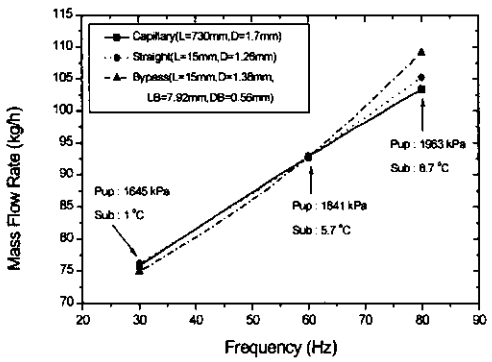

Fig. 9 Comparison of characteristics of tested expansion devices.

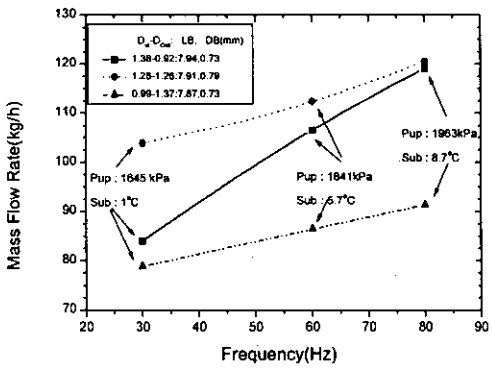

Fig. 10 Effects of tapering direction on mass flow rate.

Table 3 Coefficients of correction factors in the flow model.

Equations	Coefficients	R-22
Eq. (2)	a_1	0.02706
	a_2	11.35237
	a_3	-0.68358
	a_4	1.17439
	a_5	1.31613
	a_6	0.11144
	a_7	-0.3044
	a_8	0.67779
	a_9	0.0829
	a_{10}	0.04805
	P_c	4973.8 kPa
	T_c	369.3 K
	g_c	1.2960×10^{10}

quency is greater than those of the others, because the flashing and pressure recovery inside the orifice occur early by reducing the flow area. Therefore, tapering toward the exit of the bypass orifice is more effective on the flow rate control over a wide range.

4. Semi-empirical flow model of bypass orifices

In the present study, a mass flow model of R-22 flow through bypass orifices was developed at steady state, adiabatic, and choked flow condition when the downstream pressure was lower than saturated pressure according to the inlet temperature. The flow model was derived from the single-phase orifice equation.

$$\dot{m}_s = CA\sqrt{2\rho g_c (P_{up} - P_f)} \qquad (1)$$

where, P_f was the adjusted downstream pressure before the flashing occurred.

Correction factor, P_f was correlated with respect to each operating parameters and bypass orifice geometry. The correlation between the correction factor and the normalized parameters was determined using the non-linear regression technique along with the experimental data. All coefficients included in this flow model are given in Table 3.

$$\begin{aligned} P_f = P_{sat}[\, & a_1 + a_2(P_{up}/P_c)^{a_3}(D/D_{ref})^{a_4} \\ & SUBC^{a_5} + a_6(P_{up}/P_c)^{a_7} \\ & + a_8 \mathrm{EXP}(a_9(D/D_{ref})) \\ & + a_{10} EVAP] \end{aligned} \qquad (2)$$

where

$$PRA = P_{up}/P_c$$

$$DR = D/D_{ref}$$

$$SUBC = (T_{sat} - T_{up})/T_c$$

$$EVAP = (P_c - P_{down})/P_c$$

Normalized parameters of PRA, DR, SUB, and EVAP represent upstream pressure, diameter, subcooling, and downstream pressure, respectively. The maximum difference between the measured data and the model's prediction was within a 5%.

5. Conclusions

In the present study, the bypass orifice was designed in order to improve the performance of the inverter heat pump at high and low frequency levels of the compressor. The characteristics of the bypass orifice were measured by varying the operating conditions and geometries. The flow model for the bypass orifice was developed. As a result, the following conclusions were derived.

(1) The bypass orifice has the same flow

trends as the straight orifice. Choked flow was observed in the bypass orifice, and it would provide system reliability.

(2) The slope of mass flow rate for the bypass orifice as a function of frequency was greater than that of the straight orifice or the capillary tube.

(3) It is possible to control the variation of slope of mass flow rate of the bypass orifice according to the frequency of the compressor by changing the orifice geometries.

(4) The semi-empirical flow model was developed to predict the mass flow rate of bypass orifices with given conditions and orifice geometry. The maximum difference between the measured data and the model's prediction was within ±5%.

Acknowledgements

This work was supported by a grant No. 99-E-ID03-P-01 from Energy Conservation Foundation, Korea Energy Management Corporation.

Reference

(1) Benton, R., 1982, "Heat pump setback: computer prediction and field test verification of energy savings with improved controls", ASHRAE Journal, pp. 23-29.

(2) Lorentzen, G., 1986, "Heat pumps-where are improvements possible? An exercise in energy", International J. of Refrigeration Vol. 9, pp. 105-107.

(3) Choi, J.M., Kim, Y.C., Kim, J.Y., Bae, Y. D., 1997, "An experimental study on the performance of inverter heat pump with a variation of frequency and capillary size", SAREK Trans., Vol. 9, Part 1, pp. 64-72.

(4) Aaron, A.A., Domanski, P.A., 1989, "An experimental investigation and modeling of the flow rate of refrigerant 22 through the short tube restrictor", NIST-IR 89-4120, US Department of Commerce, NIST.

(5) Kim, Y., 1993, "Two-phase flow of HCF C-22 and HFC-134a through short tube orifices", Ph.D. Dissertation, Texas A&M University.

(6) Kim, Y.C., Choi, J.M., 1995 "Performance of capillary tubes and short tube orifices", Proceeding of the SAREK Annual Winter Conference, pp. 242-247.

(7) Kuehl, S.J., Goldschmidt, V.W., 1991, "Modeling of steady flows of R-22 through capillary tubes : test data", ASHRAE Transactions. Vol. 97, Part 1, pp. 139-148.

(8) Kim, C.N., Hwang, U.P., Park, Y.M., 1995, "Investigation of the performance of capillary tube with the roughness effect", Proceeding of the SAREK Annual Summer Conference, pp. 283-289.

(9) Han, C. S., 1991, "Computer simulation and experimental studies on the transient performance of a small refrigeration system during start-up", Ph.D Thesis, Korea Univ.